Quaternary Science Reviews
October 2019, Volume 222, Pages 105854 (7p.)
https://doi.org/10.1016/j.quascirev.2019.07.036
https://archimer.ifremer.fr/doc/00511/62289/

Carbon and silica megasink in deep-sea sediments of the Congo terminal lobes

Rabouille C. [1, *] , Dennielou Bernard [2], Baudin F. [3], Raimonet M. [4], Droz Laurence [5], Khripounoff Alexis [6], Martinez P. [7], Mejanelle L. [8], Michalopoulos P. [9], Pastor Lucie [6], Pruski A. [8], Ragueneau Olivier [4], Reyss J.-L. [1], Ruffine Livio [2], Schnyder J. [3], Stetten E. [3], Taillefert M. [10], Tourolle Julie [6], Olu Karine [6]

[1] Laboratoire des Sciences du Climat et de l'Environnement, UMR CEA-CNRS-UVSQ 8212 et IPSL, Université Paris-Saclay, Avenue de la Terrasse, 91190, Gif sur Yvette, France
[2] Unité de Recherche Géosciences Marines, IFREMER, 29280, Plouzané, France
[3] Institut des Sciences de la Terre de Paris, Sorbonne Université, CNRS, UMR 7193, 4 Place Jussieu, 75005, Paris, France
[4] Laboratoire des Sciences de l'Environnement Marin, UMR UBO-CNRS, Institut Universitaire Européen de la Mer, 29280, Plouzané, France
[5] Laboratoire Domaines Océaniques, UMR UBO-CNRS6538, Institut Universitaire Européen de la Mer, 29280, Plouzané, France
[6] IFREMER Centre Bretagne, Unité de Recherche Etude des Ecosystèmes Profonds, (REM-EEP-LEP), 29280, Plouzané, France
[7] Environnements et Paléoenvironnements Océaniques et Continentaux, Université de Bordeaux, UMR 5805, Allée Geoffroy St Hilaire, 33615, Pessac Cedex, France
[8] Laboratoire d'Ecogéochimie des Environnements Benthiques, Sorbonne Université, CNRS, UMR 8222, Observatoire Océanologique, 66650, Banyuls-sur-Mer, France
[9] Institute of Oceanography, Hellenic Center for Marine Research, 46.7 km Athens-Sounion An, Anavyssos, 19013, Greece
[10] School of Earth and Atmospheric Sciences, Georgia Institute of Technology, 311 Ferst Dr., Atlanta, GA, 30332, USA

* Corresponding author : C. Rabouille, email address : rabouill@lsce.ipsl.fr

Abstract :

Carbon and silicon cycles at the Earth surface are linked to long-term variations of atmospheric CO2 and oceanic primary production. In these cycles, the river-sea interface is considered a biogeochemical hotspot, and deltas presently receive and preserve a major fraction of riverine particles in shallow water sediments. In contrast, periods of glacial maximum lowstand were characterized by massive exports of sediments to the deep-sea via submarine canyons and accumulation in deep-sea fans. Here, we calculate present-day mass balances for organic carbon (OC) and amorphous silica (aSi) in the terminal lobe complex of the Congo River deep-sea fan as an analogue for glacial periods. We show that this lobe complex constitutes a megasink with the current accumulation of 18 and 35% of the OC and aSi river input, respectively. This increases the estimates of organic carbon burial by 19% in the South Atlantic Ocean in a zone representing less than 0.01% of the basin. These megasinks might have played a role in carbon trapping in oceanic sediments during glacial times.

Highlights

► Sediments located at the termination of Congo Canyon are a megasink of organic carbon (0.35 TgC/yr) and aSi (0.11 TgSi/yr). ► These sediments store in the deep-sea at 5 km depth 18 and 35% of Congo River OC and amorphous silica inputs, respectively. ► OC burial in these sediments increases OC burial in the South Atlantic deep basin (>3000m) by 19% for a surface area <0.01%. ► Burial efficiencies in this megasink are 85% for OC and 73% for aSi.

Keywords : Present, Paleoceanography, South Atlantic, Inorganic geochemistry, Organic geochemistry, Sedimentology-marine cores

1 Introduction

The carbon cycle regulates atmospheric CO_2 concentration, the major driver of climate variations over different timescales (Cox et al., 2000; Frank et al., 2010; Parrenin et al., 2013). Over the last

decade, the coastal ocean, and particularly large river estuaries and deltas, have received increased attention as a biogeochemical hotspot at the interface between the oceanic and continental carbon cycles (Battin et al., 2009; Bauer et al., 2013; Bianchi et al., 2014; Regnier et al., 2013). The silicon cycle is tightly linked to the carbon cycle (Tréguer et al., 2018) with diatom production and export largely contributing to the biological carbon pump and the transfer of particulate carbon from the surface to the deep ocean (Ragueneau et al., 2002). The major role of continent-ocean transfer in the marine silicon cycle has also been recognized (Tréguer and De La Rocha, 2013). As these two cycles are largely intertwined, it is of prime importance to investigate their interaction at the continent-ocean interface (Demaster, 2002; Laruelle et al., 2009).

Eustatic sea-level change is a major forcing on continent-ocean sediment transfer and submarine deep-sea fan development as it controls the location of sediment deposition on the shelf during highstands or its delivery to the deep ocean during lowstands (Posamentier and Vail, 1988; Shanmugam and Moiola, 1982; Vail et al., 1977). Though a strict lowstand model of submarine fan development is frequently discussed (Allin et al., 2017; Covault and Graham, 2010; Covault and Fildani, 2014), sea level remains the main control in areas characterized by a large continental shelf like for the Amazon fan (Flood and Piper, 1997), Mississippi (Bouma et al., 1989), Rhone fan (Lombo Tombo et al., 2015) or Danube fan (Constantinescu et al., 2015). In the present highstand ocean, terrestrial particulate organic carbon (OC) and amorphous silica (aSi) are mainly buried and recycled in river deltas (Berner, 1989; Bianchi and Allison, 2009; Bianchi et al., 2014; Blair and Aller, 2012; Burdige, 2005; Hedges and Keil, 1995; Lansard et al., 2009) and continental shelves (80-90%; (Rabouille et al., 2001), and a small fraction of riverine OC and aSi is therefore transported away to continental slopes or the abyssal plain (Canals et al.,

2006; Rabouille et al., 2009). In contrast, a larger fraction of continental carbon and silicon was transferred into canyons connected to rivers during glacial period lowstands, as rivers discharged closer to shelf breaks and slopes (Schlünz et al., 1999; Tsandev et al., 2010). As a result, the exposed continental shelf of the Amazon (Goni, 1997; Keil et al., 1997) or the Mississippi (Burdige, 2005; Newman et al., 1973) was bypassed, and deep-sea fans acted as main carbon and silicon repository during the glacial period. However, these deep-sea repositories are presently inactive making impossible to understand lowstand source-to-sink processes for OC and aSi.

The Congo River is the world's second largest river by its discharge and ranks fifth by its particulate organic carbon input to the ocean (Milliman, 1991; Spencer et al., 2014). It is the only major river directly connected to an active canyon enabling a large amount of its sediment load to bypass the shelf and to be conveyed through the canyon to the deep-sea channel-levees by turbidity current (Babonneau et al., 2002; Dennielou et al., 2017). This direct transfer thereby makes the repository zone named Congo terminal lobes (Mulder and Etienne, 2010; Savoye et al., 2009) excellent analogs to understand the functioning and the significance of river-sea fluxes of carbon and silicon in a lowstand ocean. Indeed, a large and unknown fraction of the 1.9 Tg OC y^{-1} (1Tg =10^{12} g) and 0.33 Tg aSi y^{-1} exported by the Congo River into the Atlantic Ocean is presently transported by turbidity currents over 1000 km along the submarine canyon and deep-sea channel (Azpiroz-Zabala et al., 2017; Khripounoff et al., 2003; Vangriesheim et al., 2009). Previous estimations of the organic carbon and amorphous silica accumulation in the Congo lobe complex (Rabouille et al., 2009; Raimonet et al., 2015; Stetten et al., 2015) lacked a detailed survey of the lobe complex morphology, accurate sedimentation rates, and estimates of the surface area involved to precisely determine the fate of OC and aSi. In this paper, we use a multidisciplinary dataset including detailed remotely operated vehicles (ROV) mapping,

sediment characteristics and composition together with sedimentation rates over the last century, *in situ* benthic chamber fluxes, and sediment traps to quantify the fate of deposited OC and aSi in the Congo lobe complex. This leads to the calculation of a mass balance (burial and recycling) of terrestrial OC and aSi for the lobe complex. We further estimate the proportion of terrestrial amorphous silica and organic carbon from the Congo River trapped in the terminal lobes sink and the importance of this previously unknown C and Si sink in the South Atlantic Ocean for the present and extrapolate to the glacial periods.

2. Materials and Methods

2.1. Location and background

The present Congo fan lobe complex includes five successive amalgamated lobes developed during the last 4000 years (Dennielou et al., 2017; Picot, 2015). Annual and powerful turbidity currents feeding the lobe complex have been recorded and monitored in the canyon (Heezen et al., 1964) and the deep-sea channel (Azpiroz-Zabala et al., 2017; Khripounoff et al., 2003; Vangriesheim et al., 2009), but the flux of sediment to the lobe complex is difficult to estimate because of the pulsed and unpredictable nature of these turbidity currents. Sediments record the deposition of these currents as exemplified by the counting of turbidites in sediment cores from the lobe complex combined with ^{210}Pb chronology which shows that the recurrence time of deposits by turbidity currents ranges between 6 and 17 years (Dennielou et al., 2017; Picot, 2015).

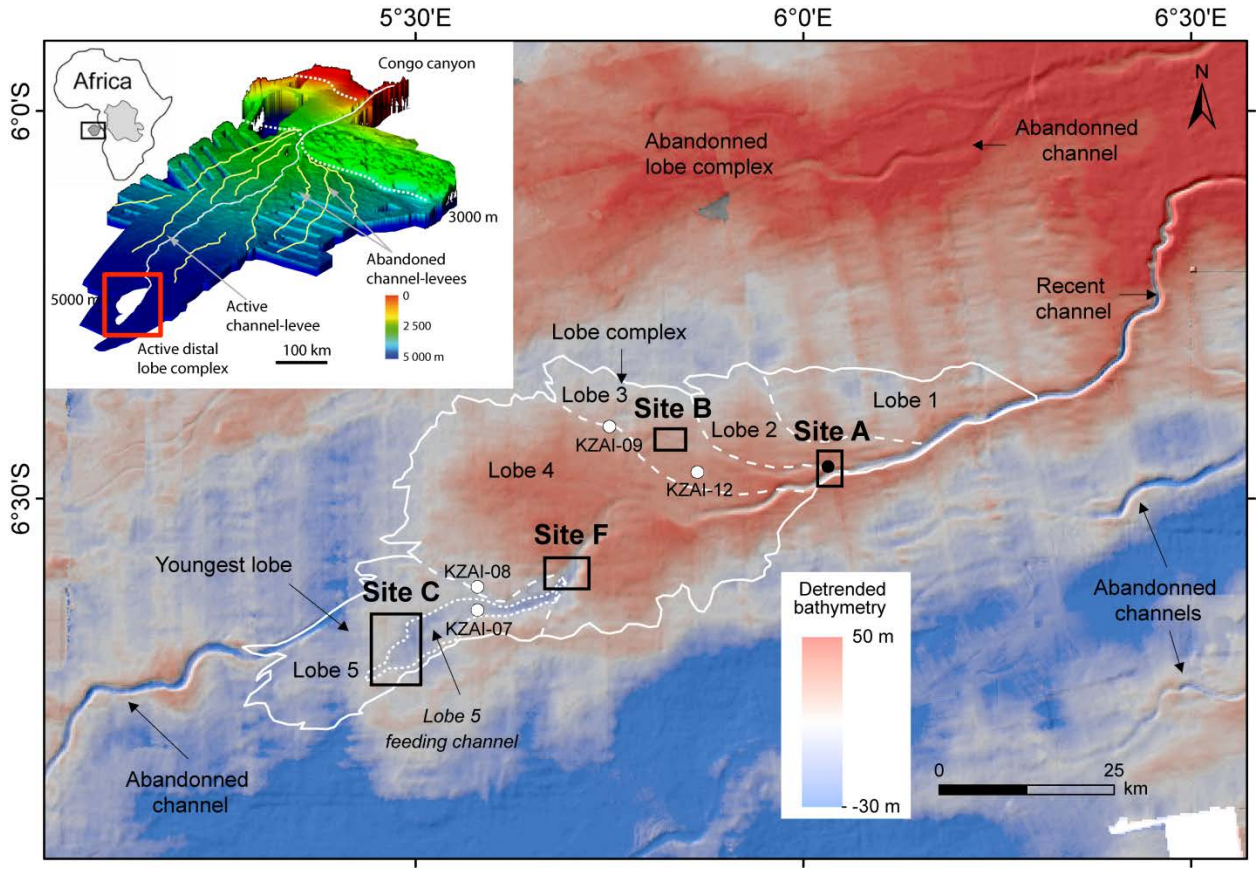

Fig.1: *Map and high resolution detrended bathymetry of the terminal lobes of the Congo deep-sea fan showing the contours of lobes numbered from 1 to 5 according to their distance from the entrance of the lobe complex (=recent channel). Average depth is 4800m (Congolobe group, 2017). Stations were located at four representative sites along the lobes (A=Lobe 1+Lobe 2, B=Lobe 3, F=Lobe 4, C=Lobe 5). The dotted line contour outlines the lobe 5 feeding channel that shows the highest sedimentation rates. White dots show the location of sediment cores used for additional sedimentation rate calculation. The black dot on Site A shows the location of sediment traps deployed in 2011.*

2.2. Methods for mass balance

Two expeditions were carried out in February 2011 (Olu, 2011) and December 2011 (Rabouille, 2011). State of the art methods were used for assessing mass balances in the terminal lobes of the Congo deep-sea fan. Most data were already published in several papers (see section 3 for references) except sediment trap fluxes, DSi benthic fluxes and aSi sediment content

(methods in Supplementary Material). Recycling rates of OC and aSi were calculated from *in situ* measurements of total oxygen uptake (TOU) and dissolved silica (DSi) benthic fluxes with a benthic chamber lander (Khripounoff et al., 2006). Uncertainty on TOU values was calculated from variability among 3 chambers during the same deployment (5-10%) and was propagated as relative uncertainty to the DSi flux. In order to recalculate OC mineralization rates, a C/O_2 (C/O_2 = 1-2*N/C; Van Cappellen and Wang, 1996) molar ratio of 0.9 was used corresponding to the average observed C/N of 15-20 observed in the area (Stetten et al., 2015). The aSi dissolution rates were assumed similar to measured dissolved silica fluxes. Burial was estimated by multiplying the measured sedimentation rates by porosity and the organic carbon or amorphous silica content (Congolobe group et al., 2017; Stetten et al., 2015; Raimonet et al., 2015) with an uncertainty calculated using 30% variability on sedimentation rates and 5% for the average OC (Baudin et al., 2017a; Baudin et al., 2017b; Stetten et al., 2015) or aSi (Raimonet et al., 2015) concentrations (see Supplementary Material for details) . Vertical fluxes of OC and aSi were measured in 2011 (unpublished data) using sediment traps deployed at 35 m above sea floor for a year at the Congolobe site without any noticeable turbidity current (Supplementrary Material). Therefore, sediment traps have measured the ambient "non-turbiditic" vertical flux. Another sediment trap array was deployed in a nearby site in 2003-2004 (site Bio-D, 200 km east of the lobe complex; Rabouille et al., 2009). In addition, a particular effort was made to estimate the lobe complex perimeter and surface areas of the five lobes using multibeam acoustic backscatter and sub-bottom profiler imagery (Dennielou et al., 2017; and Supplementary Materials).

In this paper, we used the classical method for calculating the input of OC and aSi to the lobe complex by summing independent estimates of recycling and burial fluxes (Burdige, 2006):

Input to the lobe complex = recycling flux + burial flux (Eq. 2)

As sedimentation rates were calculated from ^{210}Pb chronologies, covering a period of time of about a century (Congolobe group, 2017), the burial timescale encompasses several turbidity events (return time of 6-17 years), and is thus a fair estimate of average burial. Furthermore, since turbiditic activity in the lobe zone was absent throughout 2011 as recorded by sediment traps, we can reasonably assume that recycling is not biased by a pulse input of new turbiditic material and fairly reflects recycling between turbidity events. The OC and aSi total input fluxes were thus computed using the sum of recycling and burial fluxes for each lobe multiplied by its surface area. They were summed to determine the total inputs of OC and aSi to the lobe complex.

3 Results: cycling and burial fluxes in the terminal lobe system

3.1 Recycling of OC and aSi derived from benthic chamber measurements

TOU and DSi fluxes ranged between 5.4 and 9.6 mmol O_2 m^{-2} d^{-1} and between 0.6 and 1.9 mmol Si m^{-2} d^{-1} respectively at the different stations along the lobe complex (Table 1; Olu et al., 2017; Raimonet et al., 2015). TOU fluxes were up to one order of magnitude higher than those recorded in the South Atlantic tropical abyssal plain (0.5-1 mmol O_2 m^{-2} d^{-1}; Wenzhöfer and Glud, 2002), whereas the DSi fluxes were comparable to fluxes measured in the Equatorial Atlantic (Ragueneau et al., 2009).

Table 1: *Recycling, burial and vertical fluxes for OC and aSi in Congo lobe sediments. Recycling fluxes of OC (mineralization) and aSi (dissolution) was calculated from TOU (total oxygen uptake) and DSi flux (dissolved silica flux). Conversion of TOU to OC mineralization was made using a molar ratio C/O_2 of 0.9 (see text). Burial fluxes were calculated from measured sedimentation rates, porosity and average OC and aSi content of surface sediments (0-20cm). For recycling and burial, a weighted average for the entire lobe complex was calculated using the proportion of surface area of each lobe (see below). The measured porosity values*

190 *were averaged for depth in core between 10 and 40 cm. Vertical fluxes are from station A*
191 *(unpublished when unmarked). The mark (*) values are from Rabouille et al. (2009) and*
192 *Ragueneau et al. (2009) measured at site Bio-D 200km East of the Lobe zone at 400m above*
193 *seafloor.*

	Site A (Lobes1&2)	Site B (Lobe 3)	Site F (Lobe 4)	Site C levee (Lobe 5)	Site C channel (Lobe 5 feeding channel)	Weighted average
Recycling						
Surface area (km^2)	533	283	1203	424	82	
TOU (mmol O_2 m^{-2} d^{-1})	5.4±0.5	7±0.9	6.5±0.7	7.8±0.4	9.6±0.8	
OC miner (g C m^{-2} y^{-1})	21±2	28±4	26±3	31±2	38±4	**26±4**
DSi flux (mmol Si m^{-2} d^{-1})	1.1±0.1	-	1.9±0.2	0.6±0.1	0.6±0.1	
aSi dissol. (g Si m^{-2} y^{-1})	7.7±0.7	-	19±2	6.2±0.6	5.9±0.6	**13±2**
Burial						
Sedim. rate (cm y^{-1})	1±0.3	0.3±0.1	0.7±0.2	0.7±0.2	12±6	
Porosity	0.84	0.84	0.85	0.85	0.87	
OC (% dw)	3.25±0.2	3.2±0.2	3.3±0.2	3.4±0.2	4.0±0.2	
aSi (%Si dw)	1.3±0.1	0.9±0.1	1.2±0.1	1.2±0.1	1.0±0.1	
OC Burial (g C m^{-2} y^{-1})	130±40	38±12	87±30	89±32	1560±540	**139±42**
aSi Burial (g Si m^{-2} y^{-1})	53±11	11±4	32±8	31±9	381±125	**45±11**
OC/aSi burial (mol/mol)	5.8	8.0	6.3	6.7	9.6	**7.1**
Vertical flux						
F-aSi (g Si m^{-2} y^{-1})	1.5-2.5*					
F-OC (g C m^{-2} y^{-1})	1.1-1.7*					

194

3.2 Burial flux of OC and aSi in terminal lobe complex sediments

High sedimentation rates due to the deposition of turbidites (0.5-1 cm y^{-1}; Congolobe group et al., 2017; Rabouille et al., 2009) were recorded over the entire lobe complex. The feeding channel of lobe 5 (the most distal and recent lobe) displayed sedimentation rate of 12 cm y^{-1} (Table 1). The sedimentation rates were on average three to four orders of magnitude higher than those in the surrounding abyssal plain (Congolobe group et al., 2017; Mollenhauer et al., 2004; Stetten et al., 2015). The lobe complex sediments were characterized by large OC concentrations of OC (Stetten et al., 2015; Baudin et al., 2017b), exceeding 3% as compared to 0.5% in the Atlantic sediments of the central basin (Mollenhauer et al., 2004). In turn, aSi concentrations (0.9-1.3% Si dry weight; Raimonet et al., 2015) were in the same range as those in the abyssal plain sediments of Eastern Equatorial Atlantic (Ragueneau et al., 2009). As recently proposed by Rahman et al. (2016), aSi concentrations in lobe sediments may have been underestimated by a factor of 2-3, because of amorphous silica alteration in the shelf repository (canyon head) before being entrained by turbidity current. Burial of OC and aSi in terminal lobe sediments showed extremely large fluxes of 38-1560 g C m^{-2} y^{-1} for OC burial and 11-381 g Si m^{-2} y^{-1} for aSi (Table 1). These fluxes exceeded South Atlantic Basin values at these depths (>3000m) by a factor of 2000 for OC (0.06 g C m^{-2} y^{-1}; Mollenhauer et al., 2004) and 100 for aSi (maximum 0.4 g Si m^{-2} y^{-1}; Geibert et al., 2005). OC and aSi burial fluxes were the highest in the feeding channel of lobe 5 (station C, Fig. 1), where sedimentation rates are highest (12 cm y^{-1}; Congolobe group et al., 2017). The OC/aSi molar ratios in buried particles (average 7.1) were also consistently high (Table 1), with values that are five times larger than the maximal ratio measured in deep-sea sediments (0.02-1.7; Ragueneau et al., 2002).

3.3 Vertical flux of OC and aSi from sediment traps

The particulate OC and an aSi rain rate were much lower than the recycling and burial fluxes (Table 1). The OC/aSi molar ratio of the rain rate was 1-2, a much lower value than the measured burial ratio (≈7, Table 1) which was consistent with deep-sea sediment and trap particles OC/aSi ratio (Ragueneau et al., 2002).

4 Discussion: Budgets, burial efficiencies and comparison to riverine and marine sources

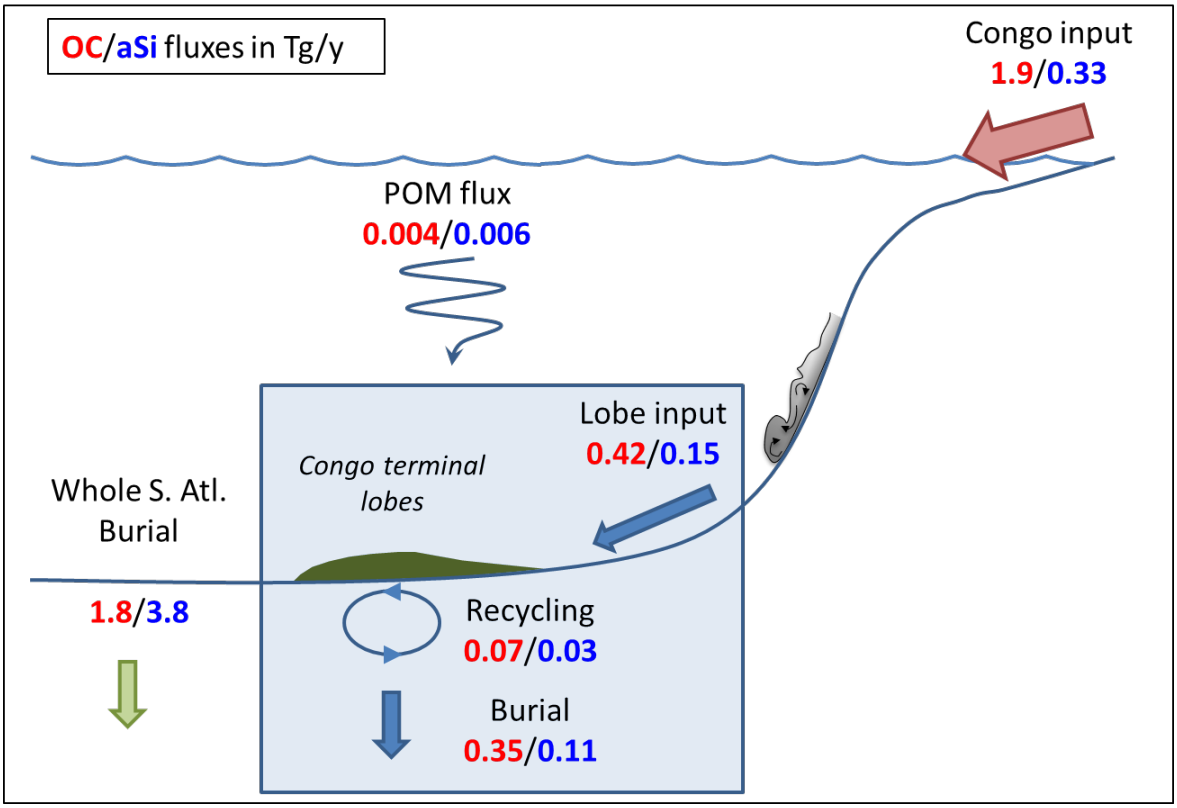

Figure 2: *Mass balance for the Congo terminal lobe complex for organic carbon (OC in Tg C y^{-1}; 1 Tg = 10^{12} g) and amorphous silica (aSi in Tg Si y^{-1}). Input from the Congo River, from the marine rain and burial rates in the South Atlantic basin (0-40°S) are also displayed. Red numbers are for OC and blue for aSi.*

The striking point of these OC and aSi budgets is the high burial rates (0.35 Tg C y^{-1} and 0.11 Tg Si y^{-1}) and the large burial efficiencies (70-85%) compared to abyssal plain sediments, where

generally only <10% of the OC and aSi rain rates are buried (Burdige, 2007; Ragueneau et al., 2002). In addition, the strong decoupling from the vertical marine flux (1% and 4% of the total OC and aSi input, Table 2) is clear. Previous results have highlighted the terrestrial nature of the lobe complex organic matter (Baudin et al., 2017b; Schnyder et al., 2017; Stetten et al., 2015). The small contribution of marine inputs to the total input corroborates the dominance of canyon inputs to the lobe complex. The comparison of the OC/aSi signature of the buried particulate matter (7.1) to the two possible sources of material (riverine=13 and marine=1.5) also points to the Congo River as the main source of sediments in the lobe complex, with limited decoupling between carbon and silicon during the transfer of particles to the terminal lobes. The OC/aSi decrease of riverine material from 13 to 7 can probably be attributed to preferential recycling of carbon versus silica (Ragueneau et al., 2002) in surficial sediments before burial (Raimonet et al., 2015). Overall, the rapid transfer of Si and C through the canyon leads to an enhanced preservation of Si and C with little decoupling (Raimonet et al., 2015) compared to the strong decoupling occurring during particle settling in the open ocean (Ragueneau et al., 2002). If generalized during glacial periods, this rapid transfer to the deep sea fans through the canyons, may lead to a decrease of biogenic matter deposition and recycling on continental shelves and slopes with the following consequences: long-term decrease of CO_2 production during mineralization of the organic matter, and short term changes of phytoplankton dynamics (diatoms) linked to lower silicic acid recycling from shelves and slopes sediments.

The present estimate of OC inputs to the lobe complex (0.42 Tg C y^{-1}) can be compared with recent estimates of canyon particulate export rates (0.5-1.1 Tg C y^{-1}) based on ADCP measurements of canyon turbidity currents at 2000 m water depth, 500 km upstream from the lobe complex (Azpiroz-Zabala et al., 2017). These comparable export rates between two distant

sites indicates that the sediment transport along the canyon and deep-sea channel is very efficient and that a significant fraction (up to 50%) of the material transported by turbidity currents may reach the lobe complex located at the far end of the channel-levee system.

Table 2: *Mass balance for the terminal lobes of the Congo deep-sea fan and comparison to the marine particulate fluxes, Congo discharge and burial in the South Atlantic (1 Tg = 10^{12} g). *aSi burial in the South Atlantic is calculated from the regional organic carbon burial and OC/aSi ratio or downscaling global fluxes (see supplementary material). OC/aSi is calculated as molar ratio compared to mass fluxes for OC and aSi.*

	OC (Tg C y^{-1})	aSi (Tg Si y^{-1})	OC/aSi (mol/mol)
Burial	0.35 ± 0.12	0.11 ± 0.05	7.1
Mineralization/dissolution	0.07 ± 0.01	0.03 ± 0.01	
Lobe input based on mass balance	**0.42 ± 0.14**	**0.15 ± 0.05**	**8.0**
Burial efficiency (BE)	84%	73%	
Marine input	0.004	0.006	1.5
% marine in total input	1%	4%	
River discharge (Coynel et al., 2005; Hugues et al., 2011; Seylers et al., 2005)	1.9	0.33	13
% burial of Congo River export	18%	35%	
Burial in deep South Atlantic (0-40°S; >3000m; (Mollenhauer et al., 2004)	1.8	3.8*	1
% burial in Congo lobes relative to deep South Atlantic	19%	3%	

The Congo lobe complex represents an overlooked sink for organic carbon and amorphous silica in the abyssal Atlantic Ocean. The OC and aSi budgets in the lobe complex are dominated by burial fluxes, 3-4 orders of magnitude larger than those in the surrounding abyssal plain (38-1560 versus 0.06 g C m^{-2} y^{-1} and 11-381 versus 0.15 g Si m^{-2} y^{-1}). When compared to the overall burial of OC in the South Atlantic (0-40°S) during the Holocene (Mollenhauer et al., 2004), the accumulation of OC in Congo terminal lobe sediments adds 19% to the estimation of OC burial in this deep ocean basin. This contribution is remarkable given the lobe area represents less than 0.01% of the South Atlantic surface area (0-40°S) and indicates that the Congo lobe complex constitutes a megasink of OC in the South Atlantic which was clearly overlooked in previous

studies due to the lack of knowledge on Congo terminal lobes. Although slightly less acute, 3% of the total burial of aSi in the South Atlantic occurs in the lobe complex. This number could be raised to 4-6% if aSi was underestimated as suggested by Rahman et al. (2016). Burial fluxes of this dominantly terrestrial OC (70-90%; Schnyder et al., 2017; Stetten et al., 2015) and aSi, that represent 18% and 35% of the Congo River discharge of POC and aSi, respectively, are in the same range of estimates for deltaic sediments, i.e. 22% of river OC input preserved (Burdige, 2005; Hedges and Keil, 1995). The estimated burial of terrigenous OC in the lobe complex (0.3 Tg C y^{-1}) represents about 0.7% of the overall terrestrial OC burial in the global abyssal ocean (Schlünz and Schneider, 2000).

The present-day export to the abyssal depth of Congo River sediments through the presently active connection to its canyon, and therefore of embedded OC and aSi, is similar to the lowstand functioning of major deep-sea fans (Vail et al., 1977), e.g. Amazon fan (Flood and Piper, 1997). It may therefore be a representative glacial analogue for terrestrial OC and aSi export when rivers discharged at the shelf break and active canyons carried a large proportion of their load to the continental rise and abyssal plain (Schlünz et al., 1999). If, as suggested in previous studies (Burdige, 2005), the same fraction of the carbon load (18%) of other major tropical rivers of the Atlantic such as the Amazon (5 Tg C y^{-1}; Moreira-Turcq et al., 2003) or the Orinoco Rivers (1 Tg C y^{-1}; Mora et al., 2014) was buried in the deep Atlantic basin during glacial times, this burial flux would equal the present-day carbon preservation in the entire South Atlantic basin and significantly increase the global oceanic carbon sink during these low CO_2 periods. The OC burial estimate for the Amazon fan during glacial times (3.7 Tg C/yr; Schlünz et al., 1999) clearly substantiate this calculation. These megasinks may also contribute to enhance OC storage during glacial by better preservation (burial efficiencies of 85%, Table 2) as

proposed by Cartapanis et al. (2016). These findings emphasize the need to better constrain these localized but intense megasinks in order to understand the natural sinks in the carbon and silica cycles during both modern and glacial times.

5 Conclusions

In this paper, we have shown that the terminal lobes of the Congo deep-sea fan constitute a singular point in the South Atlantic Ocean corresponding to a mega burial site for organic carbon and amorphous silica. It represents 19% of the entire burial of the South Atlantic Ocean for OC despite covering less than 0.01‰ of the total surface area. By comparing burial in lobe sediments with the Congo River input, we conclude that 18% of organic carbon inputs and 35% of amorphous silica inputs from the Congo River are buried in sediments, which thus constitutes a major repository for exported riverine material. This is largely due to the present and active connection of the Congo canyon to the River estuary. This situation may represent a fair analogue to glacial period river export when most rivers were closely connected to their canyons due to the low sea level. It is expected that burial of OC and aSi in these terminal lobe regions of other rivers was much larger at this period.

Conflict of interest

The authors state that there are no real or perceived conflicts of interests neither financial nor institutional.

Data

Original data were all published with the original papers (see references in text) or are contained in the Supplementary Material. The entire dataset is currently being deposited in the SEANOE data base (IFREMER).

Acknowledgments

The authors thank the captains and crews of the RV Pourquoi Pas? And the ROV teams during the WACS and Congolobe cruises. We thank two external reviewers (D. Conley, J.E. Cloern) who kindly provided useful comments to this paper. We acknowledge funding from ANR Congolobe (ANR Blanc SIMI5-6, no.11BS56030), from IFREMER (Project "Biodiversité et dynamique des écosystèmes profonds, impacts"), from CEA through LSCE (to CR) and from the U.S. National Science Foundation Chemical Oceanography Program (OCE-0831156 to MT).

References

Allin, J. R., Hunt, J. E., Clare, M. A., & Talling, P. J. (2017). Eustatic sea-level controls on the flushing of a shelf-incising submarine canyon, *GSA Bulletin*, *130*, 222-237, doi: https://doi.org/10.1130/B31658.1.

Azpiroz-Zabala, M., Cartigny, M. J. B., Talling, P. J., Parsons, D. R., Summer, E. J., Clare, M. A., Simmons, S. M., Cooper, C., & Pope, E. L. (2017). Newly recognized turbidity current structure can explain prolonged flushing of submarine canyons, *Sci. Adv.*, *3*, e1700200, doi: 10.1126/sciadv.1700200.

Babonneau, N., Savoye, B., Cremer, M., & Klein, B. (2002). Morphology and architecture of the present canyon and channel system of the Zaire dees-sea fan, *Mar. Petrol. Geol.*, *19*, 445-467.

Battin, T. J., Luyssaert, S., Kaplan, L. A., Aufdenkampe, A. K., Richter, A., & Tranvik, L. J. (2009). The boundless carbon cycle, *Nature Geoscience*, *2*, 598-600.

Baudin, F., Martinez, P., Dennielou, B., Charlier, K., Marsset, T., Droz, L., & Rabouille, C. (2017a). Organic carbon accumulation in modern sediments of the Angola basin influenced by the Congo deep sea fan, *Deep-Sea Res. II: Top. Stud. Oceanorgr.*, *142*, 64-74.

Baudin, F., Stetten, E., Schnyder, J., Charlier, K., Martinez, P., Dennielou, B., & Droz, L. (2017b). Origin and distribution of the organic matter in the distal lobe of the Congo deep-sea fan – A Rock-Eval survey, *Deep-Sea Res. II: Top. Stud. Oceanorgr.*, *142*, 75-90.

Bauer, J. E., Cai, W. J., Raymond, P. A., Bianchi, S. T., Hopkinson, C. S., & Regnier, P. A. G. (2013). The changing carbon cycle of the coastal ocean, *Nature*, *504*, 61-70.

Berner, R. A. (1989). Biogeochemical cycles of carbon and sulfur and their effect on atmospheric oxygen over phanearozoic time, *Pal. Pal. Pal.*, *73*, 97-122.

Bianchi, S. T., & Allison, M. A. (2009). Large-river delta-front estuaries as natural ‘‘recorders’’ of global environmental change, *Proc. Nat. Acad. Sci., 106*, 8085–8092.
Bianchi, S. T., Allison, M. A., & Cai, W. J. (2014), Biogeochemical dynamics at major river-coastal interfaces: linkages with Global Change, 649 pp., Cambridge University Press, New York.
Blair, N. E., & Aller, R. C. (2012). The fate of terrestrial organic carbon in the marine environment, *Ann. Rev. Mar. Sci., 4*, 401-423, doi: doi.org/10.1146/annurev-marine-120709-142717. .
Bouma, A. H., Coleman, J. H., Stelting, C. E., & Kohl, B. (1989). Influence of relative sea level changes on the construction of the Mississippi fan, *Geo-Marine Letters, 93*, 161-170, doi: https://doi.org/10.1007/BF02431043.
Burdige, D. J. (2005). Burial of terrestrial organic matter in marine sediments: A re-assessment, *Glob. Biogeochem. Cycles, 19*, GB4011, doi: doi:10.1029/2004GB002368.
Burdige, D. J. (2006), Geochemistry of marine sediments, 609 pp., Princeton University Press, Princeton, USA.
Burdige, D. J. (2007). Preservation of Organic Matter in Marine Sediments: Controls, Mechanisms and an Imbalance in Sediment Organic Carbon Budgets?, *Chem. Rev., 107*, 467-485, doi: http://dx.doi.org/10.1021/cr050347q.
Canals, M., Puig, P., Durrieu de Madron, X., Heussner, S., Palanques, A., & Fabres, J. (2006). Flushing submarine canyons, *Nature, 444*, doi:10.1038/nature05271.
Cartapanis, O., Bianchi, D., Jaccard, S.L. and Galbraith, E.D. (2015) Global pulses of organic carbon burial in deep-sea sediments during glacial maxima. Nature Comm. 7:10796.
Congolobe group, et al. (2017). The Congolobe project, a multidisciplinary study of Congo deep-sea fan lobe complex: Overview of methods, strategies, observations and sampling, *Deep-Sea Res. (II) Topic. Stud. in Oceanogr., 142*(7-24).
Constantinescu, A. M., Toucanne, S., Dennielou, B., Jorry, S. J., Mulder, T., & Lericolais, G. (2015). Evolution of the danube deep-sea fan since the last glacial maximum: New insights into Black Sea water-level fluctuations, *Mar. Geol., 367*, 50-68, doi: http://dx.doi.org/10.1016/j.margeo.2015.05.007.
Covault, J. A., & Graham, S. A. (2010). Submarine fans at all sea-level stands: Tectono-morphologic and climatic controls on terrigenous sediment delivery to the deep sea, *Geology, 38*, 939-942, doi: https://doi.org/10.1130/G31081.1.
Covault, J. A., & Fildani, A. (2014), Continental shelves as sediment capacitors or conveyors: source-to-sink insights from the tectonically active Oceanside shelf, southern California, USA, edited, p. 315, Geological Society of London Memoirs.
Cox, P. M., Betts, R. A., Jones, C. D., Spall, S. A., & Totterdell, I. J. (2000). Acceleration of global warming due to carbon-cycle feedbacks in a coupled climate model, *Nature, 408*, 184-187.
Demaster, D. J. (2002). The accumulation and cycling of biogenic silica in the Southern Ocean: revisiting the marine silica budget, *Deep-Sea Research II, 49*, 3155-3167.
Dennielou, B., et al. (2017). Morphology, structure, composition and build-up processes of the active Congo channel-mouth lobe complex with inputs from remotely operated underwater vehicle (ROV) multibeam and video surveys, *Deep-Sea Res. (II): Top. Stud.Oceanogr., 142*, 25-49.
Flood, R. D., & Piper, D. J. W. (1997). Amazon fan sedimentation: the relationship to equatorial climate change, continental denudation, and sea-level fluctuations, *Proceedings of the Ocean Drilling Program, Scientific Results, 155*, 653-675.
Frank, D. C., Esper, J., Raible, C. C., Buntgen, U., Trouet, V., Stocker, B., & Joos, F. (2010). Ensemble reconstruction constraints on the global carbon cycle sensitivity to climate, *Nature, 463*, 527-230, doi: doi:10.1038/nature08769.
Geibert, W., Rutgers van Der Loeff, M. M., Usbeck, R., Gersonde, R., Kuhn, G., & Seeberg-Everfeldt, J. (2005). Quantifying the opal belt in the Atlantic and southeast Pacific sector of the Southern Ocean by means of 230Th normalization, *Glob. Biogeochem. Cycle, 19*, GB4001, doi: doi:10.1029/2005GB002465.
Goni, M. A. (1997), Records of terrestrial organic matter composition in Amazon Fan sediments in Proceedings of the Ocean Drilling Program-Scientific Results, edited by R. D. Flood, D. J. W. Piper and L. C. Peterson, pp. 519-530, Ocean Drill. Program, College Station, Tex.
Hedges, J. I., & Keil, R. G. (1995). Sedimentary organic matter preservation: an assessment and speculative synthesis, *Mar. Chem., 49*, 81-115.
Heezen, B. C., Menzies, R. J., Schneider, E. D., Ewing, W. M., & Granelli, N. C. L. (1964). Congo Submarine Canyon, *AAPG Bulletin, 48*, 1126–1149.
Keil, R. G., Tsamakis, E. C., Wolf, N., Hedges, J. I., & Goni, M. A. (1997), Relationships between organic carbon preservation and mineral surface area in Amazon Fan sediments (Holes 932A and 942A), in Proceedings of the

Ocean Drilling Program-Scientific Results, edited by R. D. Flood, D. J. W. Piper and L. C. Peterson, pp. 531-538, Ocean Drill. Program, College Station, Tex.

Khripounoff, A., Caprais, J., Crassous, P., & Etoubeau, J. (2006). Geochemical and biological recovery of the disturbed seafloor in polymetallic nodule fields of the Clipperton-Clarion Fracture Zone (CCFZ) at 5,000-m depth, *Limnol. Oceanogr.*, *51*, 2033-2041.

Khripounoff, A., Vangriesheim, A., Babonneau, N., Crassous, P., Savoye, B., & Dennielou, B. (2003). Direct observation of intense turbidity current activity in the Zaire submarine valley at 4000 m water depth, *Mar. Geol.*, *194*, 151-158.

Lansard, B., Rabouille, C., Denis, L., & Grenz, C. (2009). Benthic remineralization at the land-ocean interface: A case study of the Rhone River (NW Mediterranean Sea), *Estuarine Coastal and Shelf Science*, *81*(4), 544-554, doi: 10.1016/j.ecss.2008.11.025.

Laruelle, G. G., et al. (2009). Anthropogenic perturbations of the silicon cycle at the global scale: Key role of the land-ocean transition, *Glob. Biogeochem. Cycle*, *23*, GB4031, doi: doi:10.1029/2008GB003267.

Lombo Tombo, S., Dennielou, B., Berné, S., Bassetti, M. A., Toucanne, S., Jorry, S. J., Jouet, G., & Fontanier, C. (2015). Sea-level control on turbidite activity in the Rhone canyon and the upper fan during the Last Glacial Maximum and Early deglacial, *Sediment. Geol.*, *323*, 148-166, doi: http://dx.doi.org/10.1016/j.sedgeo.2015.04.009.

Milliman, J. D. (1991), Flux and fate of fluvial sediment and water in coastal seas, in Ocean margin processes in global change, edited by R. F. C. Mantoura, J-M. Martin and R. Wollast, pp. 69-91, J. Wiley and sons, Berlin.

Mollenhauer, G., Schneider, R. R., Jennerjahn, T., Muller, P. J., & Wefer, G. (2004). Organic carbon accumulation in the South Atlantic Ocean: its modern, mid-Holocene and last glacial distribution, *Glob. Planet. Change*, *40*, 249-266.

Mora, A., Laraque, A., Moreira-Turcq, P., & Alfonso, J. A. (2014). Temporal variation and fluxes of dissolved and particulate organic carbon in the Apure, Caura and Orinoco rivers, Venezuela, *South Amer. J. Earth Sci. , 54*, 47-56, doi: http://dx.doi.org/10.1016/j.jsames.2014.04.010.

Moreira-Turcq, P., Seyler, P., Guyot, J. L., & Etcheber, H. (2003). Exportation of organic carbon from the Amazon River and its main tributaries, *Hydrol. Process.*, *17*, 1329–1344, doi: DOI: 10.1002/hyp.1287.

Mulder, T., & Etienne, S. (2010). Lobes in deep-sea turbidite systems: State of the art, *Sediment. Geol.*, *229*, 75-80, doi: 10.1016/j.sedgeo.2010.06.011.

Newman, J. W., Parker, P. L., & Behrens, E. W. (1973). Organic carbon ratios in Quaternary cores from the Gulf of Mexico, *Geochim. Cosmochim. Acta*, *37*, 225– 238.

Olu, K. (2011). WACS cruise, R/V Pourquoi Pas?, doi: http://dx.doi.org/10.17600/11030010.

Olu, K., Decker, C., Pastor, L., Caprais, J. C., Khripounoff, A., Morineaux, M., Ain Baziz, M., Menot, L., & Rabouille, C. (2017). Cold-seep-like macrofaunal communities in organic- and sulfide-rich sediments of the Congo deep-sea fan, *Deep-Sea Res. (II) Topic. Stud. in Oceanogr.*, *142*, 180-196.

Parrenin, F., Masson-Delmotte, V., Kohler, P., Raynaud, D., Paillard, D., Schwander, J., Barbante, C., Landais, A., Wegner, A., & Jouzel, J. (2013). Synchronous change of atmospheric CO_2 and antarctic temperature during the last deglacial warming, *Science*, *339*, 1060-1063, doi: DOI: 10.1126/science.1226368.

Picot, M. (2015), Cycles sédimentaires dans le système turbiditique du Congo: nature et origine (Doctorat Thesis). Université de Bretagne Occidentale, Brest, 368., 368 p pp, Université de Bretagne Occidentale, Brest.

Posamentier, H. W., & Vail, P. R. (1988), Eustatic Controls on Clastic Deposition II—Sequence and Systems Tract Models, in Sea-Level Changes: An Integrated Approach, edited by C. K. W. e. al., SEPM Society for Sedimentary Geology,.

Rabouille, C. (2011). CONGOLOBE cruise, R/V Pourquoi Pas? , doi: http://dx.doi.org/10.17600/11030170.

Rabouille, C., Mackenzie, F., & Ver, L. M. (2001). Influence of the human perturbation on carbon, nitrogen and oxygen biogeochemical cycles in the global coastal ocean, *Geochim. Cosmochim. Acta*, *65*, 3615-3639.

Rabouille, C., Caprais, J. C., Lansard, B., Crassous, P., Dedieu, K., Reyss, J. L., & Khripounoff, A. (2009). Organic matter budget in the Southeast Atlantic continental margin close to the Congo Canyon: In situ measurements of sediment oxygen consumption, *Deep-Sea Research Part Ii-Topical Studies in Oceanography*, *56*(23), 2223-2238, doi: 10.1016/j.dsr2.2009.04.005.

Ragueneau, O., Dittert, N., Pondaven, P., Treguer, P., & Corrin, L. (2002). Si/C decoupling in the world ocean : is the Southern Ocean different?, *Deep-Sea Res. II*, *49*, 3127-3154.

Ragueneau, O., Regaudie-de-Gioux, A., Moriceau, B., Gallinari, M., Vangriesheim, A., Baurand, F., & Khripounoff, A. (2009). A benthic Si mass balance on the Congo margin: Origin of the 4000 m DSi anomaly and implications for the transfer of Si from land to ocean, *Deep Sea Research Part II: Topical Studies in Oceanography*, *56*(23), 2197.

Raimonet, M., Ragueneau, O., Jacques, V., Corvaisier, R., Moriceau, B., Khripounoff, A., Pozzato, L., & Rabouille, C. (2015). Rapid transport and high accumulation of amorphous silica in the Congo deep-sea fan: a preliminary budget, *J. Mar Sys.*, *141*, 71-79.

Regnier, P. A. G., et al. (2013). Anthropogenic perturbation of the carbon fluxes from land to ocean, *Nat. Geosc.*, *6*, 597-607, doi: DOI: 10.1038/NGEO1830.

Savoye, B., Babonneau, N., Dennielou, B., & Bez, M. (2009). Geological overview of the Angola-Congo margin, the Congo deep-sea fan and its submarine valleys, *Deep Sea Research Part II: Topical Studies in Oceanography*, *56*(23), 2169.

Schlünz, B., & Schneider, R. R. (2000). Transport and terrestrial organic carbon to the oceans by rivers: re-estimating flux and burial rates, *Int. J. Earth Sci.*, *88*, 599-606.

Schlünz, B., Schneider, E. D., Muller, P. J., Showers, W. J., & Wefer, G. (1999). Terrestrial organic carbon accumulation on the Amazon deep sea fan during the last glacial sea level low stand, *Chem. Geol.*, *159*, 263–281.

Schnyder, J., Stetten, E., Baudin, F., Pruski, A., & Martinez, P. (2017). Palynofacies reveal fresh terrestrial organic matter inputs in the terminal lobes of the Congo deep-sea fan, *Deep-Sea Res. (II) Topic. Stud. in Oceanogr.*, *142*, 91-108.

Shanmugam, G., & Moiola, R. J. (1982). Eustatic control of turbidites and winnowed turbidites, *Geology*, *10*, 231-235, doi: https://doi.org/10.1130/0091-7613(1982)10<231:ECOTAW>2.0.CO;2.

Spencer, R. G. M., Stubbins, A., & Gaillardet, J. (2014), Geochemistry of the Congo River, estuary and plume, in Biogeochemical dynamics at the major river-coastal interfaces, edited by S. T. Bianchi, M. A. Allison and W. J. Cai, pp. 554-606, Cambridge Univ. Press, New York.

Stetten, E., Baudin, F., Reyss, J. L., Martinez, P., Charlier, K., Schnyder, J., Rabouille, C., Dennielou, B., Coston-Guarini, J., & Pruski, A. (2015). Organic matter characterization and distribution in sediments of the terminal lobes of the Congo deep-sea fan: evidence for the direct influence of the Congo River, *Mar. Geol.*, *369*, 182-195.

Tréguer, P., & De La Rocha, C. L. (2013). The world ocean silica cycle, *Ann. Rev. Mar. Sci.*, *5*, 477–501, doi: 10.1146/annurev-marine-121211-172346.

Tréguer, P., et al. (2018). Influence of diatom diversity on the ocean biological carbon pump, *Nat. Geosc.*, *11*, 27–37, doi: doi/10.1038/s41561-017-0028-x.

Tsandev, I., Rabouille, C., Slomp, C. P., & Van Cappellen, P. (2010). Shelf erosion and submarine river canyons: implications for deep-sea oxygenation and ocean productivity during glaciation, *Biogeosciences*, *7*(6), 1973-1982, doi: 10.5194/bg-7-1973-2010.

Vail, P. R., Mitchum, R. M., Todd, R. G., Widmier, J. M., Thompson III, S., Sangree, J. B., Bubb, J. N., & Hatelid, W. G. (1977), Seismic stratigraphy and global changes of sea level, in Seismic stratigraphy—Applications to hydrocarbon exploration, edited by C. E. Payton, pp. 49-212, American Association of Petroleum Geologists Memoir,.

Van Cappellen, P., & Wang, Y. (1996). Cycling of iron and manganese in surface sediments: a general theory for the coupled transport and reaction of carbon, oxygen, nitrogen, sulfur, iron and manganese, *Amer. J. Sci.*, *296*, 197-243.

Vangriesheim, A., Khripounoff, A., & Crassous, P. (2009). Turbidity events observed in situ along the Congo submarine channel, *Deep-Sea Res. II*, doi:10.1016/j.dsr1012.2009.1004.1004

Wenzhöfer, F., & Glud, R. N. (2002). Benthic carbon mineralization in the Atlantic: A synthesis based on in situ data from the last decade, *Deep-Sea Res. (I)*, *49*, 1255-1279.

Supplementary Material

- Oceanographic expeditions

Two expeditions were carried out on the Congo terminal lobe complex in 2011. The WACS cruise was conducted on the R.V. Pourquoi Pas? in February for a ROV survey and preliminary sampling of the area (Olu, 2011). The Congolobe cruise was conducted in December 2011-January 2012 on the R.V. Pourquoi Pas? As well for a larger scale mapping and sampling of the area (Rabouille, 2011). Four stations were investigated along the channel axis. Station A represents the entrance of the lobe complex, station B and F represents the intermediate younger lobes and station C is the present terminal repository. Near this last station, the dotted area represents a special sub-site where present sedimentation rates are the highest (>10 cm y^{-1}, Congolobe group, 2017) and corresponds to L5dl in the Tables. Two additional stations that were located further downstream (station D) and in an abandoned lobe complex 50km North of the active lobe area (Station E, Congolobe group, 2017), were investigated but are not reported in this study.

- Sediment processing:

Cores were sliced at 0.5 cm intervals in the first 2 cm, at 1 cm intervals down to 10 cm and at 2 cm intervals down to 20 cm within a few hours after collection. For aSi, sediments were stored frozen at -20°C, lyophilized and grinded before $aSiO_2$ concentration analyses. Pore waters were collected by centrifugation of sediment slices collected in a glove box for 20 min at 3500 rpm. The porewater samples were immediately analyzed for $Si(OH)_4$ concentrations. For OC, sediments were frozen on board and kept frozen until analysis. They were then oven dried (60°C) or freeze dried.

- Benthic chambers experiments

In situ benthic chamber incubations were processed using the "Respiromètre Autonome grande Profondeur" (RAP2; Khripounoff *et al.*, 2006). For each deployment, three benthic chambers of 30 cm diameter and 24 cm height were used for deployments of 24-48 hours. Oxygen optodes (Aanderaa) were inserted within each chamber to continuously record oxygen concentration, while three sampling cells located inside the chambers enabled water subsample collection (100 mL) at given times during the incubation (Olu *et al.*, 2017). Back on deck, these cells were subsampled for oxygen measurements by Winkler titration. Samples for DSi analysis were stored at 4°C until analyzed back in the laboratory.

Table SI-1: TOU and DSi fluxes in benthic chambers deployed during WACS and CONGOLOBE cruises outside dense habitats

	Operation	TOU (mmol O_2 m^{-2} d^{-1})	DSi flux (mmol m^{-2} d^{-1})
Site A	Col-RAP1	5.4 ± 0.5	1.1 ± 0.1
Site B	Col-RAP5	7.0 ± 0.9	-
Site F	Col-RAP2	6.5 ± 0.7	1.9 ± 0.2

Site C (levee)	Col-RAP3	7.8 ± 0.4	0.6 ± 0.1
Site C (Channel)	Calmar	9.6 ± 0.8	0.6 ± 0.1*

* value measured during the WACS cruise (Feb 2011) with the RAP lander (W-RAP4).

- Sediment traps

The Congolobe line was deployed during the present experiment at station A for 10 months (Feb-Dec 2011). The sediment trap (Technicap® PPS5, a conical sediment trap with a sampling aperture of 1 m² covered with a honeycomb baffle with openings of 1 cm in diameter, and equipped with 24 sampling bottles) deployed at 35 m a.b was associated with an Acoustic Doppler Current Profiler (ADCP) 300 kHz (Teledyne RD Instruments). Before deployment, sampling bottles were filled with filtered seawater and sodium borate-buffered formalin to a final concentration of 3%. Each bottle sampled during 15 days. Back on deck, samples were kept at 4°C before treatment. In the laboratory, the content of each bottle was visually examined to retrieve organisms larger than 1 mm, and rinsed with Milli-Q purified water to remove salts and formalin. Particles were then dried and crushed prior to analyses. These results can be compared with a mooring line equipped with similar trap design Technicap® PPS5 deployed for 5 years (2000-2004) on a nearby site 200km upstream the terminal lobe complex (Bioz-Site D; Rabouille *et al.*, 2009) which contained two traps located at 30 and 400 meters above bottom associated with current meters.

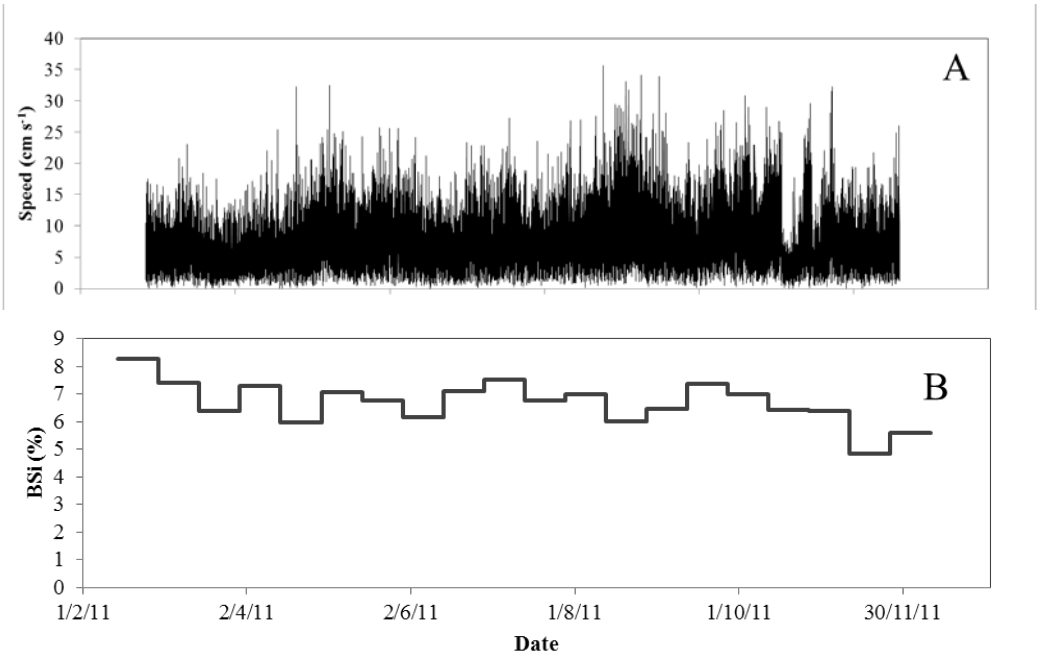

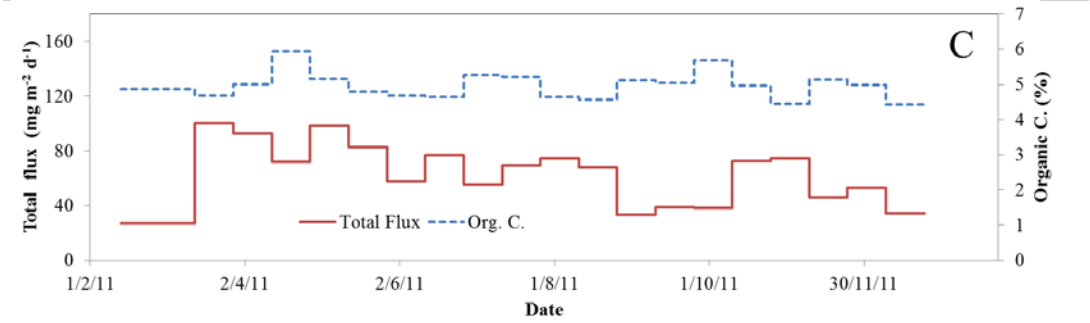

Figure SI-1 : Current measurement and particle flux at Lobe site (A: speed current, B: biogenic silica content, C: particle flux and organic carbon concentration). Original data.

Table SI-2: Average elemental composition of particles sample in the sediment trap deployed at station A from Feb to December 2011.

Site	Total flux ($mg\ m^{-2}\ d^{-1}$)	Organic C. (%)	Inorganic C. (%)	BSi (%)	N (%)	C/N
A	63.2±22.1	5.0±0.4	4.36±0.72	6.7±0.8	0.72±0.07	6.9

The calculation of annual vertical fluxes provide an average TOC flux of 1.1 g C m^{-2} y^{-1} and an average BSi flux of 1.5 g Si m^{-2} y^{-1}.

- Analytical procedures and data for aSi:

$Si(OH)_4$ concentrations in overlying and pore waters were measured following the colorimetric method of Tréguer and Le Corre (1975) modified by Aminot and Kerouel (2007). $aSiO_2$ concentrations were determined using the alkaline digestion method adapted from Köning *et al.* (2002), as described in Raimonet *et al.* (2015). The adaptation of the Aminot and Kerouel (2007) method allowed optimizing the number of $Si(OH)_4$ samples analyzed per day during the alkaline digestion.

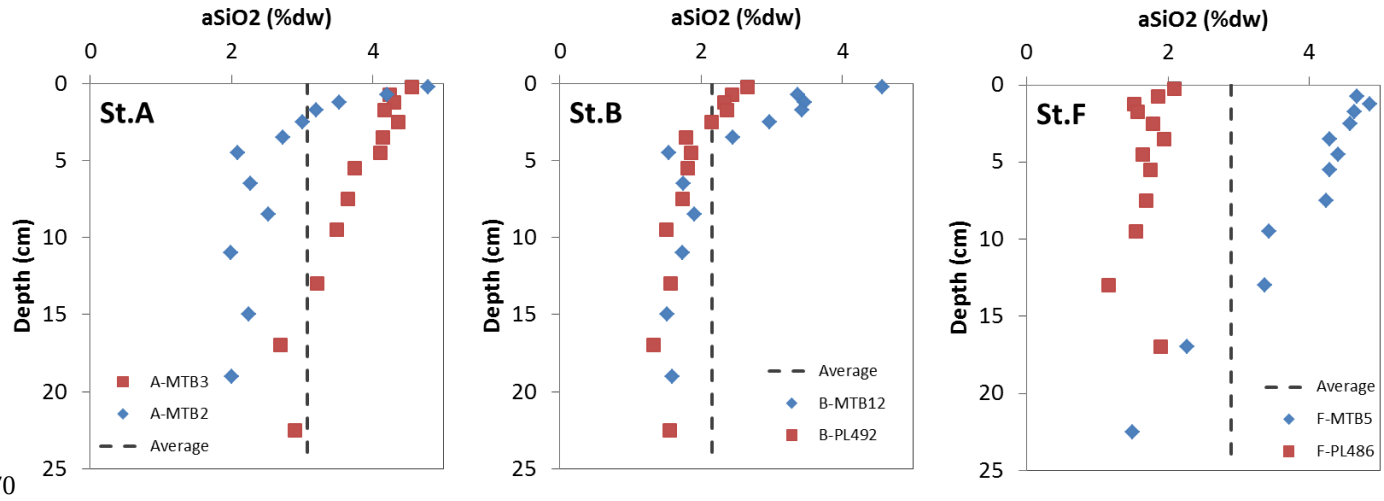

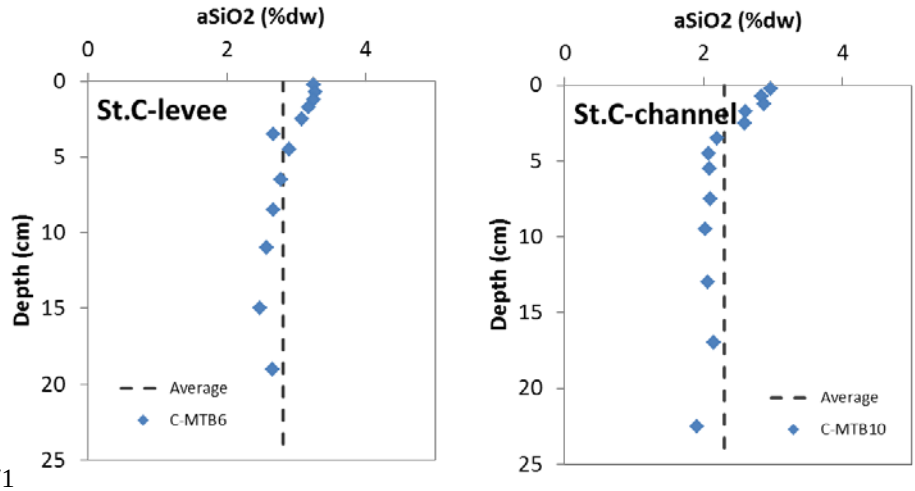

Figure SI-2: Amorphous silica distributions in Congolobe sediments reported as %aSiO2 dw (original data).

- Analytical procedures and data for OC

Total organic carbon content was measured using both a high temperature combustion method (LECO IR 212, LECO Corporation) with correction of inorganic carbon measured by carbonate-bomb and/or a pyrolytic method (Rock-Eval 6, Vinci Technologies) using a procedure devoted to recent marine sediment (Baudin *et al.*, 2015). Both methods have an analytical precision of ±0.1%. More than 475 samples were analyzed from 28 cores collected in different parts of the terminal lobes of the Congo deep-sea fan. Detailed analytical procedure and all results are reported in Stetten *et al.* (2015) and Baudin *et al.* (2017).

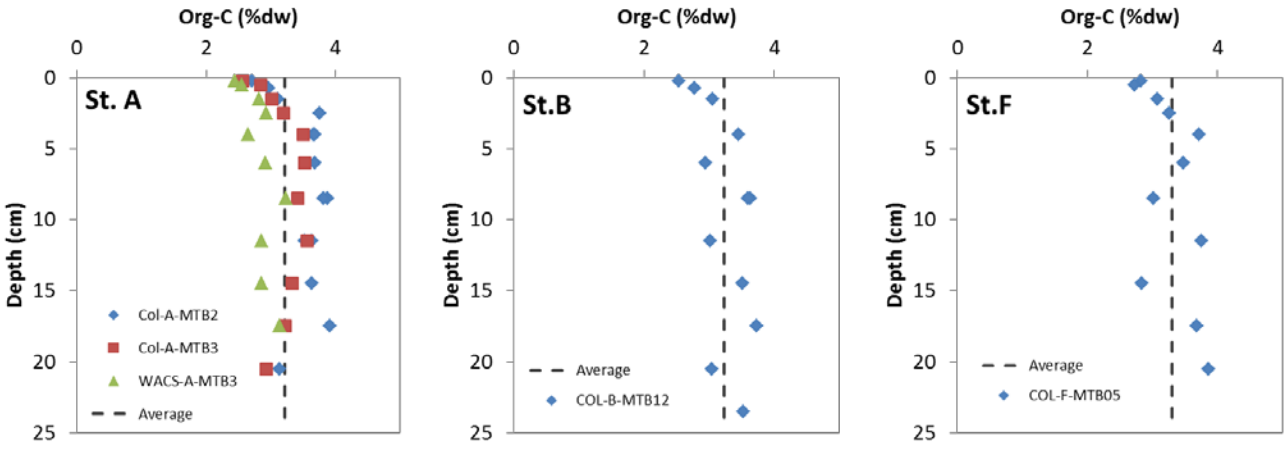

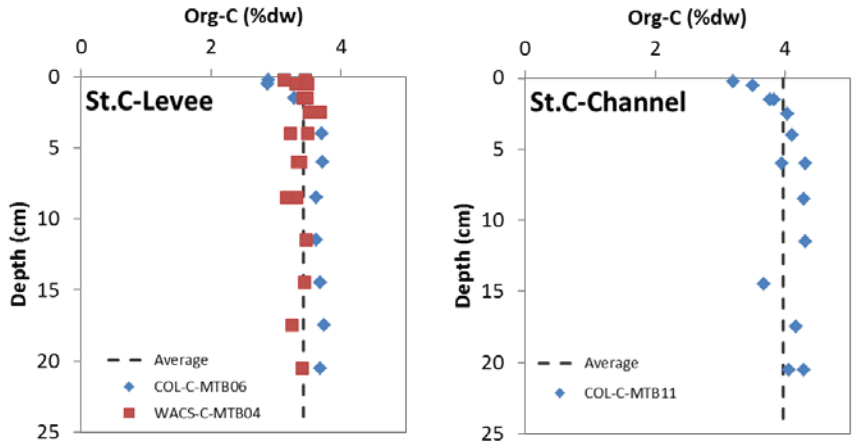

Figure SI-3: Organic carbon content in Congolobe sediments (Redrawn with permission from Stetten et al., 2015).

- Estimation of lobe complex perimeter and surface areas

The location and extension of the lobe complex of the 5 lobes was determined after multibeam acoustic backscatter and sub-bottom profilers (Dennielou *et al.*, 2017). The lobe complex corresponds to slightly convex-up morphology, mainly flat in the middle part and with steeper slopes on their sides (Mulder and Etienne, 2010). On sub-bottom profiles the lobe complex peripheral deposits show a pinch out characteristic of lateral progradation. Lobe complex deposits are characterized by disorganized high-amplitude seismic reflections that correspond to the occurrence of pervasive mass wasting. On the multibeam acoustic backscatter, the lobe complex deposits are characterized by high acoustic backscatter while the surrounding pelagic sediment of the abyssal plain is characterized by low acoustic backscatter. The lobes limits were determined after the multibeam morphology and acoustic backscatter that allowed distinguishing 5 successive prograding and overlapping lobes (for details see Dennielou et al., 2017; figures 3, 4, 5 and S2, S3, S4). On Figure 1, in order to reveal the morpho-bathymetric expression of the lobe complex, a polynomial surface corresponding to the mean slope of the area and representative of the topographic trend was calculated and then subtracted from the initial DTM (Picot *et al.*, 2016). All maps were realized with ArcGis 10.3 software, with 2 types of bathymetric data acquired during WACS (Olu, 2011) and Congolobe (Rabouille, 2011) cruises: ship bathymetry with 50/100 m of resolution and ROV bathymetry with 0.75m of resolution. The geodesic system used is a personalized Mercator projection, with standard parallel 5.5 °S and Geographic Coordinate System GCS_WGS_1984. The surface of lobes was calculated in ArcGis software with the tool "calculate geometry" directly in the attribute table with field values calculation.

- Sedimentation rates:

The sedimentation rates were assessed using short lived radionuclides $^{210}Pb^{xs}$ and ^{137}Cs methods based on interface and piston cores (see Congolobe group, 2017 for details). The short-live radionuclides were measured using gamma ray emission at LSM, a low background laboratory in

the Alps. Uncertainty on these fluxes was estimated to be 30% due to the high sedimentation rates and the short length of the cores (Congolobe group, 2017).

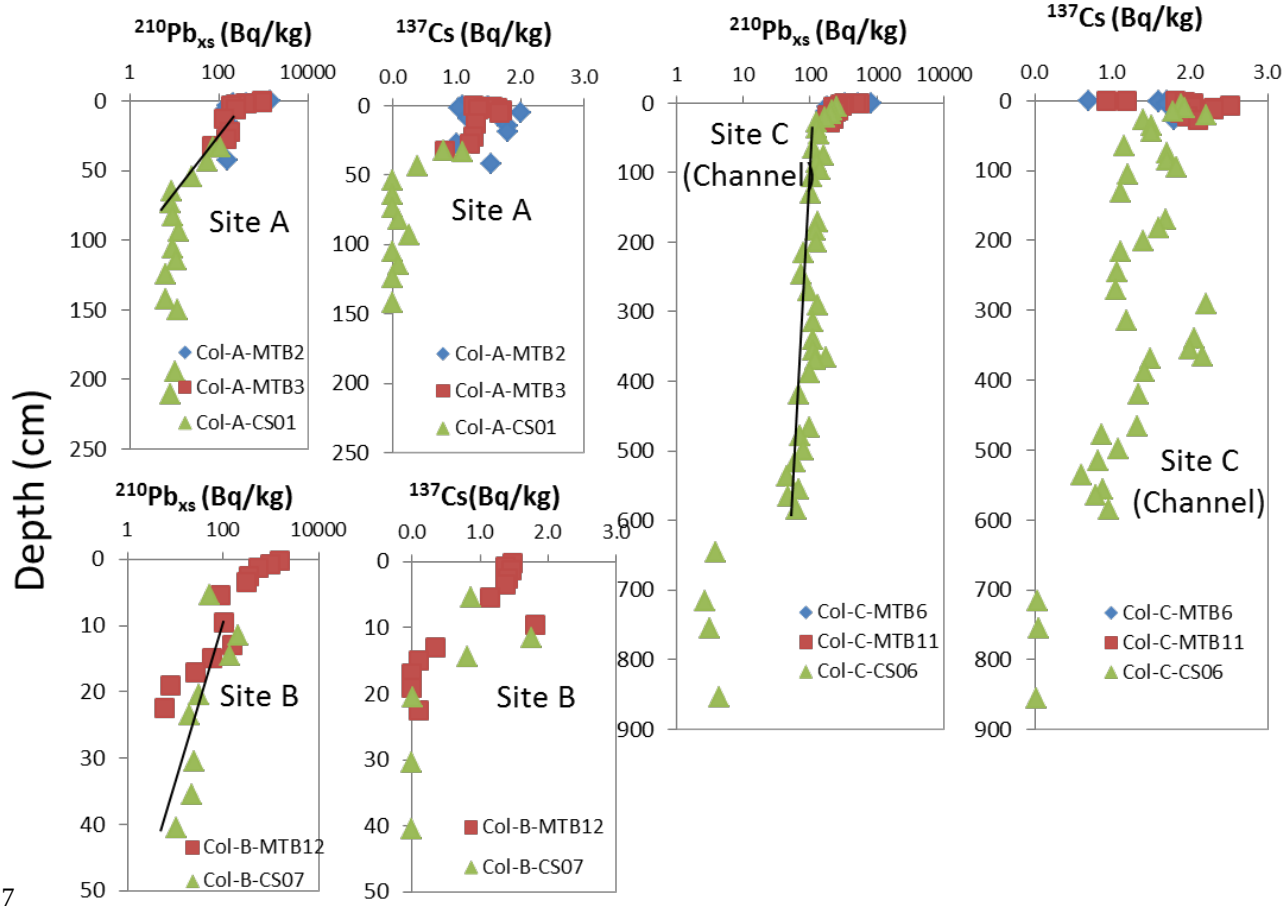

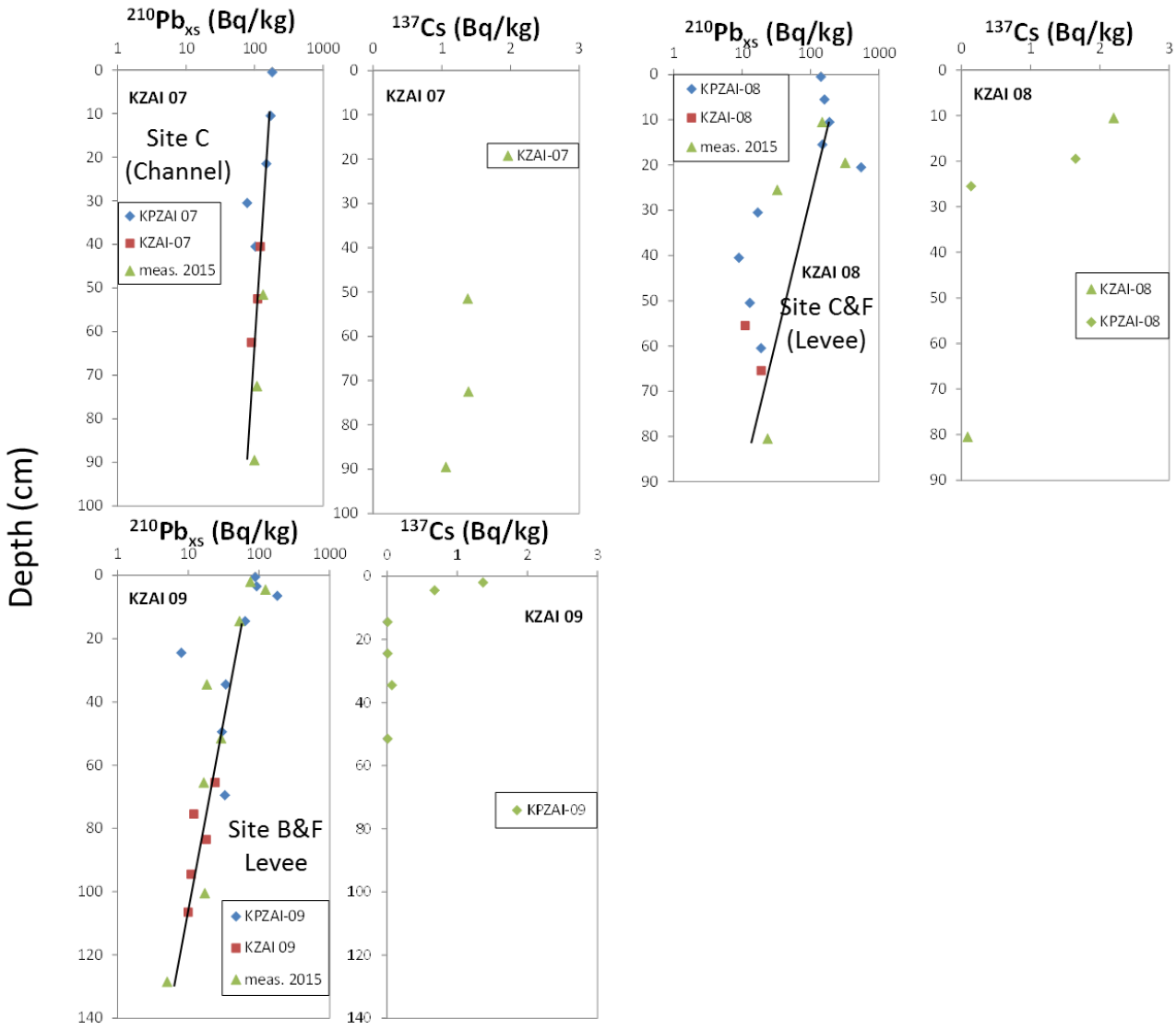

Figure SI-4: radionuclide distributions ($^{210}Pb_{xs}$ and ^{137}Cs) in Congolobe sediments (Redrawn with permission from Congolobe group, 2017).

Table SI-3: Sedimentation rates at the Congolobe/WACS/ZAIANGO sites (Redrawn with permission from Congolobe group, 2017)

Site	$^{210}Pb_{xs}$ Sedimentation rate (cm yr^{-1})	^{137}Cs Sedimentation rate (cm yr^{-1})
A	0.6	**1**
B	0.4	**0.3**
KZAI8 (C&F-levee)	0.7	**0.7**
KZAI9 (B&F-levee)	1.7	0.4
C (channel)	22	**12**
KZAI7 (C-Channel)	6.5	>2.5

- Calculations

Burial of organic carbon and amorphous silica:

OC-burial (g C m^{-2} y^{-1}) = ω * (1-Φ) * OC% *10^{-2}*2.5*10000

BSi-Burial (g Si m^{-2} y^{-1}) = ω * (1-Φ) * aSi% *10^{-2}*2.5*10000

where is ω sedimentation rate in cm y^{-1}, Φ is porosity, OC% is the organic carbon content in percent dry weight and aSi is the amorphous silica content in % Si dry weight; 2.5 is the sediment dry density in g/cm^3 and 10^{-2} and 10000 are here for unit conversion.

OC mineralization and aSi dissolution:

OCminer (g C m^{-2} y^{-1}) = (C/O_2) * TOU *365*12*10^{-3}

aSi dissol (g Si m^{-2} y^{-1}) = DSi flux*365*28*10^{-3}

where (C/O_2) is the organic carbon to oxygen ratio during mineralization taken as 0.9 equivalent to a O_2/C of 1.1 (Rabouille et al., 2009) in the lobe complex (C/N= 15-20 and C/O2 = 1–2*N/C; Van Cappellen and Wang, 1996), TOU is the oxygen demand measured by benthic chambers in mmol O_2 m^{-2} d^{-1}, DSi flux is the dissolved Si flux measured in benthic chambers in mmol Si m^{-2} d^{-1}, 28 is the molar mass of Si and 12 is the molar mass of carbon, 365 and 10^{-3} are for unit conversion.

Calculation of aSi burial for south Atlantic (0- 40°S)

Three methods were used to estimate aSi burial in South Atlantic sediment for which, to the best of our knowledge, no estimate exist in the literature.

Method 1 was based on downscaling the value proposed by Tréguer and De La Rocha (2013) for deep-sea aSi burial excluding opal rich areas to the South Atlantic. The proportion represented by the surface area of the deep South Atlantic (0- 40°S; >3000m) to the surface area of the total deep-sea (10%) was calculated and used to scale down aSi burial.

Method 2 was based on the burial flux from Geibert *et al.* (2005) who reported burial in two stations of the Polar Front Zone (PFZ) and Sub Antarctic Zone (SAZ) (around 45°S). This value was multiplied by the surface area considered in this paper (30*10^{12} m^2). It constitutes a maximal value as aSi flux and burial in the PFZ and SAZ is influenced by the opal belt and is larger than aSi burial in the subtropical gyre and tropical ocean. The burial flux of 0.4 gC m^{-2} y^{-1} (Geibert et al., 2005) is clearly not compatible with the C/Si molar ratio of 4 and a burial of OC of 0.1 gC m^{-2} y^{-1} observed in the western South Atlantic.

Method 3 is based on C/Si ratio in South Atlantic deep-sea sediments collected from three papers. They appear to differ from the East of the South Atlantic basin (Burckle, 2001; Bohrmann, 1999) to the West of the basin (Romero and Hensen, 2002). We then split the accumulation of OC between the eastern and western basin of the South Atlantic (Mollenhauer *et al.*, 2004). As no obvious pattern is visible for OC burial in the deep South Atlantic, we decided

to split it in two identical parts. We then divided each accumulation by the C/Si ratio and summed the two parts.

For the final aSi burial, we averaged method 1 and method 3, excluding method 2 which provided obviously non extrapolable and much larger results. The final result is 3.8 Tg Si y^{-1} with a probable uncertainty of 30% based on methods 1 and 3.

Method 1: based on Treguer 2013 (downscaling from global)

Total deep-sea burial (excluding opal rich sediments)	28	Tg Si y^{-1}
Surface area S. Atl. (0-40°S)	30	Mkm^2 = $30*10^{12}$ m^2
Surface area global deep-ocean	300	Mkm^2 = $300*10^{12}$ m^2
Burial S. Atl =	2.8	Tg Si /y

Method 2: based on Geibert 2005 (upscaling from SAZ)

SAZ burial =	0.4	g Si m^{-2} y^{-1}
Surface area S. Atl	30	Mkm^2 = $30*10^{12}$ m^2
Burial	12	Tg Si /y

Method 3: based on aSi/OC ratio in sediments and Mollenhauer (2004) OC burial

OC/aSi S-East Atl (Burckle-Bohrman)	0.2	gC/gSi
OC/aSi S-west Atl (Romero)	4	gC/gSi
Accumulation of OC in S. Atl	1.8	Tg C y^{-1}
East	0.9	Tg C y^{-1}
West	0.9	Tg C y^{-1}
Accumulation of aSi in S. Atl		
East	4.5	Tg Si y^{-1}
West	0.225	Tg Si y^{-1}
Burial Si S.Atl	4.7	Tg Si y^{-1}

References

Aminot, A., & Kerouel, R. (2007), Dosage automatique des nutriments dans les eaux marines: methodes en flux continu, IFREMER, Quae Editions.

Baudin, F., Disnar, J. R., Aboussou, A., & Savignac, F. (2015). Guidelines for Rock–Eval analysis of recent marine sediments, *Org. Geochem.*, *86*, 71-80.

Baudin, F., Martinez, P., Dennielou, B., Charlier, K., Marsset, T., Droz, L., & Rabouille, C. (2017). Organic carbon accumulation in modern sediments of the Angola basin influenced by the Congo deep sea fan, *Deep-Sea Res. II: Top. Stud. Oceanorgr.*, *142*, 64-74.

Bohrmann, G. (1999), Geochemistry of surface sediments from the South Atlantic, edited, PANGAEA.

Burckle, L. H. (2001), Distribution of opal in surface sediments, compiled from different sources, edited, PANGAEA.

Congolobe group, et al. (2017). The Congolobe project, a multidisciplinary study of Congo deep-sea fan lobe complex: Overview of methods, strategies, observations and sampling, *Deep-Sea Res. (II) Topic. Stud. in Oceanogr.*, *142*(7-24).

Dennielou, B., et al. (2017). Morphology, structure, composition and build-up processes of the active Congo channel-mouth lobe complex with inputs from remotely operated underwater vehicle (ROV) multibeam and video surveys, *Deep-Sea Res. (II): Top. Stud.Oceanogr.*, *142*, 25-49.

Geibert, W., Rutgers van Der Loeff, M. M., Usbeck, R., Gersonde, R., Kuhn, G., & Seeberg-Everfeldt, J. (2005). Quantifying the opal belt in the Atlantic and southeast Pacific sector of the Southern Ocean by means of 230Th normalization, *Glob. Biogeochem. Cycle*, *19*, GB4001, doi: doi:10.1029/2005GB002465.

Khripounoff, A., Caprais, J., Crassous, P., & Etoubeau, J. (2006). Geochemical and biological recovery of the disturbed seafloor in polymetallic nodule fields of the Clipperton-Clarion Fracture Zone (CCFZ) at 5,000-m depth, *Limnol. Oceanogr.*, *51*, 2033-2041.

Köning, E., Epping, E., & Van Raaphorst, W. (2002). Determining biogenic silica in marine samples by tracking silicate and aluminium concentrations in alkaline leaching solutions, *Aquat. Geochem.* , *8*, 37-67.

Mollenhauer, G., Schneider, R. R., Jennerjahn, T., Muller, P. J., & Wefer, G. (2004). Organic carbon accumulation in the South Atlantic Ocean: its modern, mid-Holocene and last glacial distribution, *Glob. Planet. Change*, *40*, 249-266.

Mulder, T., & Etienne, S. (2010). Lobes in deep-sea turbidite systems: State of the art, *Sediment. Geol.*, *229*, 75-80, doi: 10.1016/j.sedgeo.2010.06.011.

Olu, K. (2011). WACS cruise, R/V Pourquoi Pas?, doi: http://dx.doi.org/10.17600/11030010.

Olu, K., Decker, C., Pastor, L., Caprais, J. C., Khripounoff, A., Morineaux, M., Ain Baziz, M., Menot, L., & Rabouille, C. (2017). Cold-seep-like macrofaunal communities in organic- and sulfide-rich sediments of the Congo deep-sea fan, *Deep-Sea Res. (II) Topic. Stud. in Oceanogr.*, *142*, 180-196.

Picot, M., Droz, L., Marsset, T., Dennielou, B., & Bez, M. (2016). Controls on turbidite sedimentation: insights from a quantitative approach of submarine channel and lobe architecture (Late Quaternary Congo Fan), *Mar. Pet. Geol.* , *72*, 423-446, doi: http://dx.doi.org/10.1016/j.marpetgeo.2016.02.004.

Rabouille, C. (2011). CONGOLOBE cruise, R/V Pourquoi Pas? , doi: http://dx.doi.org/10.17600/11030170.

Rabouille, C., Caprais, J. C., Lansard, B., Crassous, P., Dedieu, K., Reyss, J. L., & Khripounoff, A. (2009). Organic matter budget in the Southeast Atlantic continental margin close to the Congo Canyon: In situ measurements of sediment oxygen consumption, *Deep-Sea Research Part Ii-Topical Studies in Oceanography*, *56*(23), 2223-2238, doi: 10.1016/j.dsr2.2009.04.005.

Raimonet, M., Ragueneau, O., Jacques, V., Corvaisier, R., Moriceau, B., Khripounoff, A., Pozzato, L., & Rabouille, C. (2015). Rapid transport and high accumulation of amorphous silica in the Congo deep-sea fan: a preliminary budget, *J. Mar Sys.*, *141*, 71-79.

Romero, O., & Hensen, C. (2002). Oceanographic control of biogenic opal and diatoms in surface sediments of the Southwestern Atlantic, *Mar. Geol.*, *186*, 263-280.

Stetten, E., Baudin, F., Reyss, J. L., Martinez, P., Charlier, K., Schnyder, J., Rabouille, C., Dennielou, B., Coston-Guarini, J., & Pruski, A. (2015). Organic matter characterization and distribution in sediments of the terminal lobes of the Congo deep-sea fan: evidence for the direct influence of the Congo River, *Mar. Geol., 369*, 182-195.

Tréguer, P., & De La Rocha, C. L. (2013). The world ocean silica cycle, *Ann. Rev. Mar. Sci., 5*, 477–501, doi: 10.1146/annurev-marine-121211-172346.